Attitude Control Strategies for an Imaging CubeSat

Conference Paper · July 2019

DOI: 10.1109/EIT.2019.8833806

3 authors:

Giovanni Lavezzi
South Dakota State University
1 PUBLICATION **0** CITATIONS
SEE PROFILE

Mariusz Eivind Grøtte
Norwegian University of Science and Technology
5 PUBLICATIONS **15** CITATIONS
SEE PROFILE

Marco Ciarcià
South Dakota State University
24 PUBLICATIONS **177** CITATIONS
SEE PROFILE

Attitude Control Strategies for an Imaging CubeSat

Giovanni Lavezzi*
South Dakota State University, 57006 Brookings, South Dakota
Mariusz Eivind Grøtte†
Norwegian University of Science and Technology, Trondheim, Norway
Marco Ciarcià‡
South Dakota State University, 57006 Brookings, South Dakota

***Abstract*—This paper presents two different attitude control strategies for a fixed target-tracking remote sensing CubeSat. In particular, the observation mission profile requires the CubeSat to quickly reorient itself from its initial attitude to point an imager toward a fixed target area on the Earth's surface. Subsequently, it will be required to slew to maintain a very accurate pointing of the same area for the several seconds needed for the image acquisition. We first consider a classical proportional-derivative controller based on the feedback of quaternions, representative of the satellite attitude. Secondly, we implement an advanced optimal guidance based on a direct optimization method, the Inverse Dynamics in the Virtual Domain, and a nonlinear programming solver, the Sequential Gradient-Restoration Algorithm. The key advantage of such optimal guidance is the quick calculation of minimum-time reorientation maneuver.**

***Index Terms*—Optimal Guidance, Satellite Attitude, Feedback PD Controller, Quaternions, Inverse Dynamics, Sequential Gradient Restoration Algorithm.**

I. Introduction

The vast majority of spacecraft (S/C) are frequently required to perform attitude change maneuvers along the course of their missions. For example, attitude alignment must be achieved to execute in-orbit rendezvous between two spacecraft, or a particular pointing is required to direct the thrust vector when performing translation maneuvers. Another variety of attitude maneuvers are performed by observation satellites to point their cameras toward the outer space and/or areas on the Earth's surface. A typical Earth imaging satellite points a target area for a brief single image acquisition to move to the next targets for subsequent acquisitions. Several cameras, however, need to point the same target area for a prolonged time (dozens of seconds) to acquire a series of images to synthetically increase the effective signal-to-noise ratio (SNR) and spatial resolution. Obviously, accuracy in the pointing process is a crucial requirement for Attitude Determination and Control System (ADCS) of the satellite. Moreover, a fast initial pointing is a highly desirable performance to enable the acquisition of more images in a single orbit.

*Ph.D. Candidate, Department of Mechanical Engineering, South Dakota State University (SDSU), *giovanni.lavezzi@jacks.sdstate.edu.*

†Center of Excellence for Autonomous Marine Operations and Surveillance (AMOS); Department of Engineering Cybernetics, Norwegian University of Science and Technology (NTNU), *mariusz.eivind.grotte@ntnu.no.*

‡Assistant Professor, Department of Mechanical Engineering, South Dakota State University (SDSU), *marco.ciarcia@sdstate.edu.*

Optimal control problems regarding the reorientation of a S/C have been studied assuming both minimum time and minimum energy optimization criteria. Bilimoria and Wie investigated the time optimal rest to rest reorientation of a inertially symmetric S/C with independent three-axis control, showing that the optimal solution is bang–bang in all three components and the resulting motion has a significant nutational component [7]. Typically, non optimal attitude control strategies to perform a targeting maneuvers are based on PID feedback controller (quaternion-based controls) [9][3][13] or on nonlinear attitude controllers [18][8]. Recently, the IDVD, a direct optimization method, has been applied to this kind of problems. Notably, the IDVD approximates the attitude trajectory as set of basis functions, like polynomial functions [2][15], or Bernstein polynomials together with the Bézier curves [1][14]. The resulting nonlinear programming problem is then quickly solved by the SGRA. In most cases the solution is sub-optimal, but the high computational speed, due to the limited number of free trajectory parameters, allows the IDVD-SGRA to be implemented on-board in a closed-loop fashion so to recalculate the solution trajectory as the maneuver occurs. In turn, this methodology allows to compensate for modeling inaccuracies and other disturbances.

In our scenario, the ADCS of a 6U CubeSat carrying an Earth remote sensing camera is developed and two different control strategies are analyzed. The first one is based on a feedback proportional and derivative (PD) controller based on a quaternion representation of the attitude parameters. The second one is an optimal control strategy based on the combination of the Inverse Dynamics in the Virtual Domain (IDVD) method together with the Sequential Gradient-Restoration Algorithm (SGRA). The ultimate goal is to minimize the satellite reorientation time from its initial attitude in idle mode (Cruise/Stand-by) to point the desired target, and then to follow the target for all the time required by the imager to scan and acquire the sequence of images. The CubeSat is equipped with actuators for the attitude control and sensors for the attitude determination. The scenario involves the CubeSat being deployed in a slightly eccentric Sun-synchronous Low Earth Orbit (LEO) and it will scan the target areas to detect and monitor events that may be naturally static or dynamic.

II. Scenario description

A. Reference frames and orbit characterization

In this paper, as depicted in Fig.1, four different reference frames are considered.

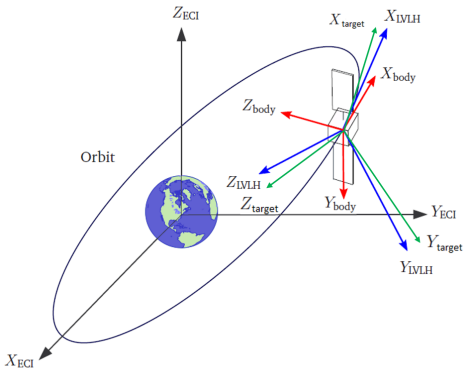

Figure 1: Reference frames (ECI, body, LVLH, Target).

The *Earth Centered Inertial* (ECI) reference frame has its origin in the center of the Earth where a Cartesian coordinate system is defined with (X_{ECI}) pointing towards the vernal equinox, (Z_{ECI}) coinciding with the north pole axis and (Y_{ECI}) perpendicular to the previous two [6]. The *Body-fixed* reference frame is a rotating reference frame centered on the center of mass of the spacecraft, with its axes parallel to the body's principal axis of inertia. The *Local-Vertical Local-Horizon* (LVLH) reference frame is centered on the spacecraft, with one axis directed toward the center of the Earth (Z_{LVLH}), another one normal to the orbital plane (Y_{LVLH}) and the last perpendicular to the previous two (X_{LVLH}), producing a right hand triad. Lastly, in order to obtain the target pointing, a *Target* reference frame centered on the spacecraft is considered, with one axis directed toward the target on the Earth surface (Z_{Target}), another one given by the cross product between Z_{Target} and S/C velocity vector (Y_{Target}) and the last perpendicular to the previous two (X_{Target}), producing a right hand triad.

The orbit of the spacecraft is a slightly eccentric Sun-synchronous Low Earth Orbit (LEO), with an orbital period of $94\,\text{min}\ 5\,\text{s}$ and with an eclipse duration equal to the 36% of the orbital period. This orbit is selected since every time that the satellite is overhead, the surface illumination angle on the planet underneath it will be nearly the same and shifts in Right Ascension of the Ascending Node (RAAN) are the least. This consistent lighting is a useful characteristic for this kind of remote-sensing satellites.

B. Perturbations

Orbital perturbations produce different torque magnitudes dependent on the orbit type and altitude selected, disturbing the attitude of the spacecraft and leading to a reduction in its pointing accuracy. Moreover, in this simulation disturbances only affect the attitude of the spacecraft (no coupling with the orbital dynamics).

During its revolution in orbit, four different orbital perturbations are taken into consideration: the atmospheric drag, the solar radiation pressure, the non-homogeneous gravitational attraction and the Earth magnetic field.

The first three disturbance torques are computed using the following expressions:

$$\boldsymbol{T}_{drag} = \begin{cases} -\frac{1}{2}\rho C_D \left\|\boldsymbol{v}_b\right\|^2 \frac{\boldsymbol{v}_b}{\|\boldsymbol{v}_b\|} \sum_{i=1}^{n} \boldsymbol{c}_i \times (\boldsymbol{n}_i \cdot \frac{\boldsymbol{v}_b}{\|\boldsymbol{v}_b\|}) A_i & (\boldsymbol{n}_i \cdot \frac{\boldsymbol{v}_b}{\|\boldsymbol{v}_b\|}) > 0 \\ 0 & (\boldsymbol{n}_i \cdot \frac{\boldsymbol{v}_b}{\|\boldsymbol{v}_b\|}) \leq 0 \end{cases} \tag{1}$$

$$\boldsymbol{T}_{srp} = \begin{cases} \sum_{i=1}^{n} \boldsymbol{c}_i \times P A_i (\boldsymbol{S}_b \cdot \boldsymbol{n}_i) \left[(1-\rho_s)\boldsymbol{S}_b + (2\rho_s(\boldsymbol{S}_b \cdot \boldsymbol{n}_i) + \frac{2}{3}\rho_d)\boldsymbol{n}_i \right] & (\boldsymbol{S}_b \cdot \boldsymbol{n}_i) > 0 \\ 0 & (\boldsymbol{S}_b \cdot \boldsymbol{n}_i) \leq 0 \end{cases} \tag{2}$$

$$\boldsymbol{T}_{grav} = \frac{3\mu}{\boldsymbol{R}^3} \begin{bmatrix} (I_z - I_y)c_3 c_2 \\ (I_x - I_z)c_1 c_3 \\ (I_y - I_x)c_1 c_2 \end{bmatrix} \quad , \quad \begin{bmatrix} c_1 \\ c_2 \\ c_3 \end{bmatrix} = \mathbf{A}_{BL} \begin{bmatrix} 0 \\ 0 \\ -1 \end{bmatrix} \tag{3}$$

- ρ: atmospheric density, assumed an exponential atmospheric model;
- C_D: drag coefficient, assumed a value equal to 2.4;
- $\boldsymbol{v}_b$: spacecraft velocity relative to the atmosphere in Body frame;
- A_i: area of each side of the CubeSat;
- $\boldsymbol{n}_i$: versor normal to each CubeSat surface;
- $\boldsymbol{c}_i$: position of the S/C centre of pressure w.r.t. the centre of mass;
- P: average solar radiation pressure, $4.6 \times 10^{-6}\ \text{N/m}^2$;
- $\boldsymbol{S}_b$: normalized distance between S/C and Sun in body frame;
- ρ_s: absorption coefficient (assumed typical value of 0.6);
- ρ_d: diffusive reflection coefficient ($\rho_d = 1 - \rho_s - \rho_a$, with $\rho_a = 0.35$);
- μ: Earth standard gravitational parameter;
- $\boldsymbol{R}^3$: S/C state position vector;
- I_x, I_y, I_z: principal axis of inertia;
- $\mathbf{A}_{BL}$: rotation matrix Body w.r.t. LVLH frame [12].

The solar radiation pressure exhibits a discontinuous effect due to the orbital eclipses, therefore a simple algorithm that detect if the spacecraft is in sunlight or in shadow is implemented.

Lastly, the Earth magnetic field is modeled starting from the magnetic potential (International Geomagnetic Reference Field - IGRF), obtaining the magnetic field in Earth-Centered Earth-Fixed (ECEF) reference frame through the negative gradient of the scalar magnetic potential, and subsequently rotating it firstly in ECI reference frame (B_x, B_y, B_z) and then in Body frame, to finally compute the magnetic torque disturbance:

$$V(\boldsymbol{r}) = a \sum_{n=1}^{k} \left(\frac{a}{r}\right)^{n+1} \sum_{m=0}^{n} (g_n^m \cos m\phi + h_n^m \sin m\phi) P_n^m(\theta) \tag{4}$$

$$\boldsymbol{B}_{r,\theta,\phi} = -\nabla V(\boldsymbol{r}) \tag{5}$$

$$\begin{cases} B_x = (B_r \cos\delta + B_\theta \sin\delta)\cos\alpha - B_\phi \sin\alpha \\ B_y = (B_r \cos\delta + B_\theta \sin\delta)\sin\alpha + B_\phi \cos\alpha \\ B_z = (B_r \sin\delta + B_\theta \cos\delta) \end{cases} \tag{6}$$

$$\boldsymbol{B}_{body} = \mathbf{A}_{BN} \boldsymbol{B}_{inert} \tag{7}$$

$$\boldsymbol{T}_{magn} = \boldsymbol{m} \times \boldsymbol{B}_{body} \tag{8}$$

- a: reference radius of the Earth (a = 6371.2 km);
- r, θ, ϕ: spherical geocentric coordinates of the spacecraft (respectively: distance from the center of the Earth, colatitude and longitude) [16];
- g_n^m, h_n^m: IGRF-2015 coefficients (up to thirteenth order);
- $P_n^m(\theta)$: Schmidt quasi-normalized associated Legendre functions of degree n and order m [16];
- δ: latitude measured positive North from the equator;
- α: local sidereal time of the location;
- $\mathbf{A}_{BN}$: rotation matrix Body w.r.t. ECI frame [17];
- $\boldsymbol{m}$: residual magnetic induction in the S/C.

C. Actuators

Reaction wheels (RW) are a type of momentum exchange devices based on acceleration and deceleration of spinning rotors, that have zero angular velocity as nominal condition. For this mission four RW in tetrahedral configuration are used. Fig.2 shows the tetrahedral configuration of four RW, whereas the specifications are reported in Tab.I, and using the following expressions it's possible to find the RW' control torque:

$$\mathbf{A} = \begin{bmatrix} \sqrt{\frac{2}{3}} & -\sqrt{\frac{2}{3}} & 0 & 0 \\ \sqrt{\frac{1}{3}} & \sqrt{\frac{1}{3}} & -\sqrt{\frac{1}{3}} & -\sqrt{\frac{1}{3}} \\ 0 & 0 & \sqrt{\frac{2}{3}} & -\sqrt{\frac{2}{3}} \end{bmatrix} \tag{9}$$

$$\dot{\boldsymbol{h}}_r = \mathbf{A}^*(\mathbf{A}\boldsymbol{h}_r \times \boldsymbol{\omega} - \boldsymbol{u}_{id}) \tag{10}$$

$$\boldsymbol{T}_{RW} = -\mathbf{A}\dot{\boldsymbol{h}}_r - (\boldsymbol{\omega} \times \mathbf{A}\boldsymbol{h}_r) \tag{11}$$

- $\boldsymbol{h}_r$: RW' angular momentum around its spin axis;
- $\mathbf{A}$: 3x4 matrix with as many columns as the number of RWs, and each column represents the direction of the axis of rotation of the wheel;
- $\mathbf{A}^*$: Moore-Penrose pseudoinverse of $\mathbf{A}$;
- $\boldsymbol{u}_{id}$: ideal control law generating the requested torque;
- $\boldsymbol{\omega}$: S/C angular velocities;
- $\boldsymbol{T}_{RW}$: RW' actuated control torque.

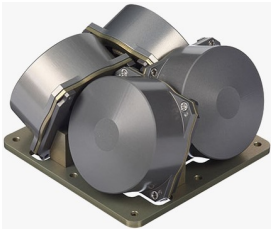

Figure 2: Example of four reaction wheels in tetrahedral configuration (source:NanoAvionics).

III. Spacecraft dynamics and attitude determination

A. Spacecraft dynamics

The orbital dynamics of the spacecraft is described by the use of equations derived from the restricted two-body problem model (R2BP), instead the computation of the attitude motion of the spacecraft is based on the unconstrained Euler equations describing the rotation of a rigid body, using the body reference frame [17]:

$$\begin{cases} I_x\dot{\omega}_x + (I_z - I_y)\omega_z\omega_y = u_x + T_x \\ I_y\dot{\omega}_y + (I_x - I_z)\omega_x\omega_z = u_y + T_y \\ I_z\dot{\omega}_z + (I_y - I_x)\omega_y\omega_x = u_z + T_z \end{cases} \tag{12}$$

where $I_{x,y,z}$ represent the inertia moments, $\omega_{x,y,z}$ are the angular velocities and $\dot{\omega}_{x,y,z}$ their derivatives, whereas $u_{x,y,z}$ and $T_{x,y,z}$ are respectively the control action and the environment disturbance torque acting on the spacecraft.

From the angular velocities it is possible to obtain, through a proper integration, the relative attitude of the spacecraft (body reference frame) with respect to the ECI reference frame; in this way the attitude kinematics is fulfilled using quaternions as attitude parameters. Quaternions are four parameters (minimum global representation), are globally defined (no singularities), and non unique:

$$\frac{\mathrm{d}\{q_0, \boldsymbol{q}\}^T}{\mathrm{d}t} = \frac{1}{2}\begin{bmatrix} 0 & -\omega_x & -\omega_y & -\omega_z \\ \omega_x & 0 & \omega_z & \omega_y \\ \omega_y & -\omega_z & 0 & \omega_x \\ \omega_z & \omega_y & -\omega_x & 0 \end{bmatrix} \{q_0(t), \boldsymbol{q}(t)\}^T \tag{13}$$

where $q_0(t)$ is the scalar component and $\boldsymbol{q}(t)$ is the vector component of the quaternions.

B. Attitude control strategies

B.1 Feedback PD controller

The desired attitude maneuver is a combination of a target pointing together with a slewing maneuver, to continuously reorient the S/C to be able to follow the target. Furthermore, the desired pointing is achieved when the S/C *Body* reference frame is aligned with the *Target* reference frame. For this reason, an attitude error may be defined as: $\boldsymbol{\varepsilon}_{att} = [\mathbf{A}_{BT}^T - \mathbf{A}_{BT}]^V$ where $\mathbf{A}_{BT}$ is a Direction Cosines Matrix (DCM) that describe the position of the body frame with respect to the Target frame; the difference of the two DCM matrices produces a skew-symmetric matrix that can be mapped to an error vector and then converted into a quaternions error vector. The ideal control law, that produces the requested torque, is based on a quaternions proportional and derivative control:

$$\boldsymbol{u}_{id} = -k_p^q \frac{\partial H(q_{0e})}{\partial q_{0e}} \boldsymbol{q}_e - k_d^q \boldsymbol{\omega}_{BT} \tag{14}$$

where $\boldsymbol{q}_e$ is the quaternions error vector, q_{0e} is the scalar component of the quaternions error vector, $H(q_{0e})$ is a function that satisfy the Lyapunov Stability theorem, whereas k_p^q and k_d^q are respectively the proportional and the derivative gains. The gains are properly selected to satisfy the time requirement (maximum settling time) and the pointing accuracy (see Tab.I).

The ideal control law is used to model the actuators and, in the case of the RW, for each of them a PI controller is used to control the motor. In particular, the wheel speed ($\boldsymbol{\omega}_{motor}$) is compared with the correspondent reference value ($\boldsymbol{\omega}_{ref}$) to produce the control action ($\boldsymbol{u}_{motor}$) according to the following PI law:

$$\boldsymbol{u}_{motor} = -k_p^m(\boldsymbol{\omega}_{motor} - \boldsymbol{\omega}_{ref}) - k_i^m \int (\boldsymbol{\omega}_{motor} - \boldsymbol{\omega}_{ref}) \tag{15}$$

where k_p^m and k_i^m are the proportional and integral gains related to the motor controller. In addition, the conversion from a continuous to a discrete response of the motor is made by using a Pulse-Width Modulation (PWM) logic on the motor voltage for wheel speed control, and for all the above cases, without loss of generality, the sampling rate chosen is $10\,\mathrm{Hz}$.

As results, it is possible to determine the actual control torque acting in the Spacecraft Dynamics (Fig.3).

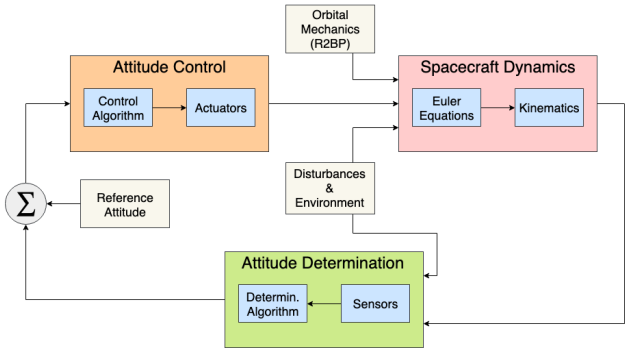

Figure 3: ADCS architecture block scheme.

B.2 IDVD-SGRA

The optimization strategy used in this work to determine the optimal attitude trajectory is the Inverse Dynamics in the Virtual Domain (IDVD), a direct method which allows to convert such optimization problem to an equivalent nonlinear programming problem, that is into a problem of minimizing a specific scalar function [4]

$$f = f(x_1, x_2, ..., x_n), \tag{16}$$

with respect to the parameters $x_1, x_2, ..., x_n$ satisfying a set of constraints

$$\boldsymbol{\phi}(x_1, x_2, ..., x_n) \leq 0. \tag{17}$$

Considering the nature of the SGRA, only equality constraints can be considered, therefore all the inequality constraints are converted into equality constraints by using an expedient, the insertion of slack variables s_i

$$\boldsymbol{\phi}_i(x_1, x_2, ..., x_n)^2 + s_i^2 = 0. \tag{18}$$

The main idea in the IDVD approach is to approximate the satellite attitude angle with a set of polynomial expressions[14][15]. For this project, the satellite attitude is represented as Euler angles (rotational sequence 1-2-3), because of the lower computational time w.r.t. other satellite attitude representations [14], and these are described in the virtual domain $\tau \in [0, 1]$ by using Bernstein polynomials together with the Bézier curves, because of their capability to approximate complex shapes through curve fitting and computational efficiency [10].

Given a set of control points $a_0, a_1, a_2, \ldots, a_s$ in $\boldsymbol{R}$, the Bézier curve $B(\tau)$ that interpolates these points is defined as [10]

$$B(\tau) = \sum_{i=0}^{p} a_i \beta_{i,p}(\tau), \tag{19}$$

where $\beta_{i,p}(\tau)$ is the pth order Bernstein polynomials

$$\beta_{i,p}(\tau) = \binom{p}{i}(1-\tau)^{p-i}\tau^i, \tag{20}$$

acting as basis form of $B(\tau)$ and $\tau \in [0, 1]$ the virtual argument. This formulation yields to the following properties at the endpoints, which are employed by IDVD to define the trajectory with the Bézier curve [1]:

1) $a(0) = a_0$ and $a(1) = a_p$;
2) $\frac{\mathrm{d}a(0)}{\mathrm{d}\tau} = p(a_1 - a_0)$ and $\frac{\mathrm{d}a(1)}{\mathrm{d}\tau} = p(a_p - a_{p-1})$.

Following this approach, each Euler angle is represented as a Bézier curve as follows:

$$\theta_j(\tau) = \sum_{i=0}^{p} a_{j,i}\beta_{i,p}(\tau), \quad \tau \in [0, 1], \quad j = 1, 2, 3 \tag{21}$$

where the coefficients $a_{j,i}$ are the control points and they are related to the boundary conditions on attitude and angular velocity, whereas $\beta_{i,p}(\tau)$ is the Bernstein polynomial base. The coefficients of these polynomials are chosen such that the initial and final conditions on the attitude and the angular velocities are automatically satisfied [4][5]. The subsequent inversion of the spacecraft dynamic allows to obtain analytical expressions of the control torque involving a limited number of parameters. Depending on the order of the Bernstein polynomial considered to describe the attitude angle, a better approximation of the attitude maneuver can be achieved.

Once the attitude is defined in the virtual domain, an additional monotonic increasing function

$$t = g(\tau), \quad \tau \in [0, 1], \tag{22}$$

must be provided to map the actual time domain $[0, t_f]$ with the virtual variable domain $[0, 1]$. For this application, we consider the polynomial expression

$$t(\tau) = \sum_{i=0}^{z} b_i^2 \tau^i, \quad \tau \in [0, 1]. \tag{23}$$

In this way, an analytical description of the spacecraft attitude motion in time domain is obtained by assigning values to the parameters $a_{j,i}$, b_i. The choice to describe the trajectory w.r.t. a virtual argument τ different than the actual time t, introduces flexibility on the solution; in fact, the values of the coefficients $a_{j,i}$ will define the attitude motion only in space, instead the parameters b_i affect also its velocity [5].

In our approach, boundary conditions related to the attitude angles and to the angular velocities at the initial and final time of the maneuver are considered. By exploiting the properties of the Bézier curve at the endpoints, for the initial conditions we have:

$$a_{j,0} = \theta_{t_0 j}, \quad a_{j,1} = \frac{\dot{\theta}_{t_0 j}}{n\lambda_{\tau t}(0)} + a_{j,0}. \tag{24}$$

and for the final conditions:

$$a_{j,p} = \theta_{t_f j}, \quad a_{j,p-1} = -\frac{\dot{\theta}_{t_f j}}{p\lambda_{\tau t}(1)} + a_{j,p}. \tag{25}$$

with

$$\frac{\mathrm{d}\theta_j(\tau)}{\mathrm{d}\tau} = \frac{\frac{\mathrm{d}\theta_j(\tau)}{\mathrm{d}t}}{\lambda_{\tau t}}, \quad \lambda_{\tau t} = \frac{1}{\frac{\mathrm{d}t}{\mathrm{d}\tau}}. \tag{26}$$

In the previous expressions, $\theta_{t_0 j}$ and $\theta_{t_f j}$ denote the jth Euler angle at the initial and final time respectively, whereas their time derivatives are retrieved performing the time derivative of the following Euler angles ($\boldsymbol{\theta} = [\theta_1, \theta_2, \theta_3]^T$) kinematic

differential equation (rotational sequence 1-2-3):

$$\boldsymbol{\theta} = \frac{1}{\cos(\theta_2)} \begin{bmatrix} \cos(\theta_3) & -\sin(\theta_3) & 0 \\ \sin(\theta_3)\cos(\theta_2) & \cos(\theta_3)\cos(\theta_2) & 0 \\ -\cos(\theta_3)\sin(\theta_2) & \sin(\theta_3)\sin(\theta_2) & 1 \end{bmatrix} \boldsymbol{\omega} \tag{27}$$

It's important to note the singularity in Eq.27 in correspondence of trajectories having $\theta_2 = \pm 90°$, condition in which the parametric curve cannot be represented because of the undetermined coefficient $a_{j,p-1}$. Although this can be a limit of the proposed algorithm, it's possible to define strategies in order to avoid this singularity condition.

No boundary conditions are imposed on the angular acceleration, however in order to find the expression of the torque in time domain, there is the need to convert $\dot{\theta}(\tau)$ in $\dot{\theta}(t)$ and $\ddot{\theta}(\tau)$ in $\ddot{\theta}(t)$ by using the following relations

$$\frac{\mathrm{d}\theta(t)}{\mathrm{d}t} = \frac{\mathrm{d}\theta(\tau)}{\mathrm{d}\tau}\lambda_{\tau t} \tag{28}$$

$$\frac{\mathrm{d}^2\theta(t)}{\mathrm{d}t^2} = \frac{\mathrm{d}^2\theta(\tau)}{\mathrm{d}\tau^2}\lambda_{\tau t}^2 + \frac{\mathrm{d}\theta(\tau)}{\mathrm{d}\tau}\lambda_{\tau t}\frac{\mathrm{d}\lambda_{\tau t}}{\mathrm{d}\tau} \tag{29}$$

The degree p of the Bézier curves in Eq.21 is related to the total number N_B of boundary conditions to be imposed on the attitude spacecraft, in particular p must satisfy the following inequality

$$p \geq N_B + 1 \tag{30}$$

In this analysis, the minimum degree is $p = 5$, and in this way at least two polynomial coefficients $a_{j,i}$ for each angle are left as variable parameters for the optimization, together with the coefficients b_i, involving flexibility on the shape of the attitude motion. As result, 5^{th} and 7^{th} degree Bernstein polynomials representing the attitude angle are considered, whereas 1^{st},2^{nd},3^{rd} and 4^{th} degree polynomials associated with the time are taken into exam.

As last step of the IDVD approach we have to invert the dynamics equation, in order to explicit the control torque

$$\begin{cases} u_x = I_x\dot{\omega}_x + (I_z - I_y)\omega_z\omega_y - T_x(t) \\ u_y = I_y\dot{\omega}_y + (I_x - I_z)\omega_x\omega_z - T_y(t) \\ u_z = I_z\dot{\omega}_z + (I_y - I_x)\omega_y\omega_x - T_z(t) \end{cases} \tag{31}$$

where the angular velocity $\boldsymbol{\omega}$ is obtained by the inversion of Eq.27, namely

$$\begin{cases} \omega_x = \cos(\theta_2)\cos(\theta_3)\dot{\theta}_1 + \sin(\theta_3)\dot{\theta}_2 \\ \omega_y = -\cos(\theta_2)\sin(\theta_3)\dot{\theta}_1 + \cos(\theta_3)\dot{\theta}_2 \\ \omega_z = \sin(\theta_2)\dot{\theta}_1 + \dot{\theta}_3 \end{cases} \tag{32}$$

whereas the angular acceleration $\dot{\boldsymbol{\omega}}$ comes from the time derivative of Eq.32. Taking into consideration all the previous relations expressed in Eqs. 21,23,24,25,26,27,28,29,32, the torque is function of the boundary conditions imposed, the extra coefficients $a_{j,i}$ the time coefficients b_i, and one independent variable τ. As results, there are all the elements to state a nonlinear programming problem as aforementioned.

The Sequential Gradient-Restoration Algorithm (SGRA) is a first-order nonlinear programming solver, developed by Angelo Miele and his research group in 1969 [11], characterized by good performances in terms of robustness and convergence speed [5]. It is based on a cyclical scheme whereby, first, the constraints are satisfied to a prescribed accuracy (restoration phase); then, using a first-order gradient method, a step is taken toward the optimal direction to improve the performance index (gradient phase). The scalar function (or objective function) f to be minimized is the maneuver time, namely

$$f = t(1) \tag{33}$$

The set of equality constraints are

$$\phi_{1,i} = u^2(t(\tau_i)) + s_{1,i}^2 - u_{max}^2 = 0 \tag{34}$$

$$\text{with} \quad \tau_i = 0 : \frac{1}{N} : 1, \quad \text{N: discretization points}$$

being $s_{1,i}$ the slack variables used to convert the inequality constraints in equality constraints. Referring to the constraints associated to the objective function, $\phi_{1,i}$ expresses that the control torque in the discretization points must be less than the maximum available u_{max}.

As result, it's possible to define the augmented function F as

$$F = f + \lambda^T\phi, \tag{35}$$

with f the performance index, λ the vector of Lagrange multipliers and ϕ the matrix of equality constraints.

In addition, we must consider the constraint error $P = \phi^T\phi$ and the optimality condition error $Q = F_x^T F_x$, being x the vector of parameters $(x_1, x_2, ..., x_n)$ and

$$F_x = \left(\frac{\partial F}{\partial x_1}, \frac{\partial F}{\partial x_2}, ..., \frac{\partial F}{\partial x_n}\right)^T \tag{36}$$

the gradient of the augmented function w.r.t. the parameters. Based on convergence studies in our simulations, the convergence conditions have been set to $P \leq 10^{-10}$ and $Q \leq 1$.

IV. Simulations and results

Table I: Simulation data and requirements.

Data	Value
S/C mass	$12\,\mathrm{kg}$
Moment inertia I_x	$13 \times 10^{-2}\,\mathrm{kg\,m^2}$
Moment inertia I_y	$10 \times 10^{-2}\,\mathrm{kg\,m^2}$
Moment inertia I_z	$5 \times 10^{-2}\,\mathrm{kg\,m^2}$
Orbit altitude	$500\,\mathrm{km}$
Orbit inclination	$97.31°$
Orbit period	$94\,\mathrm{min}\ 5\,\mathrm{s}$
Max RW torque	$\pm 3.2 \times 10^{-3}\,\mathrm{N\,m}$
Max RW momentum storage	$\pm 20 \times 10^{-3}\,\mathrm{N\,m\,s}$
Max RW DC voltage	$\pm 5\,\mathrm{V}$
Desired pointing accuracy	$\leq 0.1°$

In the simulation, four different cases of the same attitude maneuver are considered. The attitude maneuver is a combination of a minimum time target pointing together with a slewing maneuver, namely, the S/C is required to intercept the target as quickly as possible (minimum time maneuver) and to maintain the pointing within a prescribed pointing accuracy

for all the time required by the mission. The settling time of the maneuver is the performance parameter adopted to compare the results. Table I reports the simulation data and the desired requirements for the mission scenario. The four cases differ for the initial attitude considered: at the beginning of the simulation the target is assumed to be on the Earth's surface and at the same latitude and longitude coordinates of the S/C, so that the initial attitude results in the misalignment between the *Body-fixed* and the *Target* frame. For each of the four cases, two strategies are compared: the first one is characterized by the use of the feedback PD controller for the whole trajectory, whereas the second one is a combination of the IDVD-SGRA together with the same PD controller. In particular, in the second strategy, the IDVD-SGRA is exploited in an open-loop guidance fashion: at the beginning of the simulation, the predicted future initial position and attitude (without considering the external disturbances) of the S/C and of the target are given as input to the IDVD-SGRA. After the determination of the optimal solution, it will provide the torque histories necessary to the S/C to quickly re-orient itself to follow the target; after this first maneuver is completed, the residual misalignment between the S/C and the target is quasi nulled, and a commanded switch toggles the PD controller that concludes the maneuver. The aim of this strategy is to have a an efficient and computationally fast method to perform the initial interception maneuver. For the simulation, in order to reduce the computational time of the IDVD-SGRA, a 5^{th} order Bernstein polynomial and a 1^{st} order time polynomial are selected, and in this way the IDVD-SGRA is able to compute the sub-optimal trajectories in a computational time of around $10\,\text{s}$-$20\,\text{s}$ for all the cases.

A. Case 1

Table II: Case 1, data and simulation results.

Data	Value
Initial attitude (error *Body-Target*)	$[2.7°, -4.7°, 7.8°]$
Initial angular velocity	$[10^{-6}\,°/\text{s}, 10^{-6}\,°/\text{s}, 10^{-6}\,°/\text{s}]$
Settling time (PD)	$8.23\,\text{s}$ (100%)
Settling time (IDVD-SGRA+PD)	$5.88\,\text{s}$ (71.56%)

Table II reports the initial conditions and the results for the first simulation case. As shown, the minimum settling time of the maneuver is reached by the second strategy, with a settling time that is the 28.44% lower than the first strategy.

B. Case 2

Table III: Case 2, data and simulation results.

Data	Value
Initial attitude (error *Body-Target*)	$[-18.3°, 16.6°, 32.1°]$
Initial angular velocity	$[10^{-6}\,°/\text{s}, 10^{-6}\,°/\text{s}, 10^{-6}\,°/\text{s}]$
Settling time (PD)	$12.39\,\text{s}$ (100%)
Settling time (IDVD-SGRA+PD)	$11.61\,\text{s}$ (93.76%)

Table III reports the initial conditions and the results for the second simulation case. As shown, the minimum settling time of the maneuver is achieved by the second strategy, with a settling time that is the 6.24% lower than the first strategy.

C. Case 3

Table IV: Case 3, data and simulation results.

Data	Value
Initial attitude (error *Body-Target*)	$[61.6°, -23.6°, 97.0°]$
Initial angular velocity	$[10^{-6}\,°/\text{s}, 10^{-6}\,°/\text{s}, 10^{-6}\,°/\text{s}]$
Settling time (PD)	$24.51\,\text{s}$ (100%)
Settling time (IDVD-SGRA+PD)	$19.47\,\text{s}$ (79.43%)

Table IV reports the initial conditions and the results for the third simulation case. As shown, the minimum settling time of the maneuver is reached by the second strategy, with a settling time that is the 20.57% lower than the first strategy.

D. Case 4

Table V: Case 4, data and simulation results.

Data	Value
Initial attitude (error *Body-Target*)	$[56.6°, 33.2°, -153.5°]$
Initial angular velocity	$[10^{-6}\,°/\text{s}, 10^{-6}\,°/\text{s}, 10^{-6}\,°/\text{s}]$
Settling time (PD)	$30.18\,\text{s}$ (100%)
Settling time (IDVD-SGRA+PD)	$20.88\,\text{s}$ (69.18%)

Table V reports the initial conditions and the results for the fourth simulation case. As shown, the minimum settling time of the maneuver is achieved by the second strategy, with a settling time that is the 30.82% lower than the first strategy. The following figures represent the results for this case and for both the two strategies adopted, namely strategy (PD) with only the PD controller and strategy (I-S+PD) with the PD controller and the open-loop IDVD-SGRA guidance control. In particular, Fig.4 and 5 depict respectively the attitude error and the angular velocity error between the *Body* and the *Target* frame, whereas, Fig.6 shows the requested control torque, in which the maximum torque constraint is not satisfied by the PD controller. Lastly, Fig.7 and 8 show the time histories of the actuated torque components $T_{RW_{1,2,3,4}}$ for the two strategies.

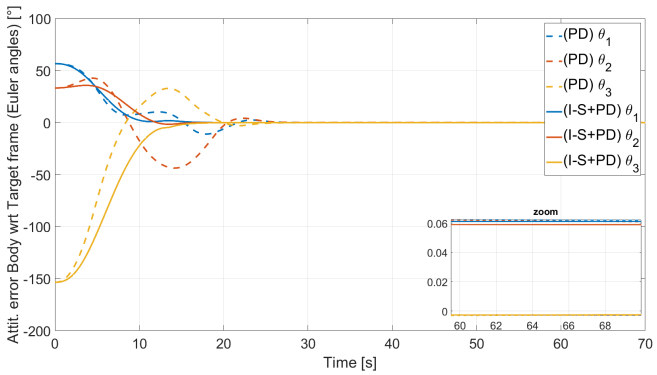

Figure 4: Case 4, attitude error Body w.r.t. Target frame. Comparison between PD and IDVD-SGRA+PD strategies.

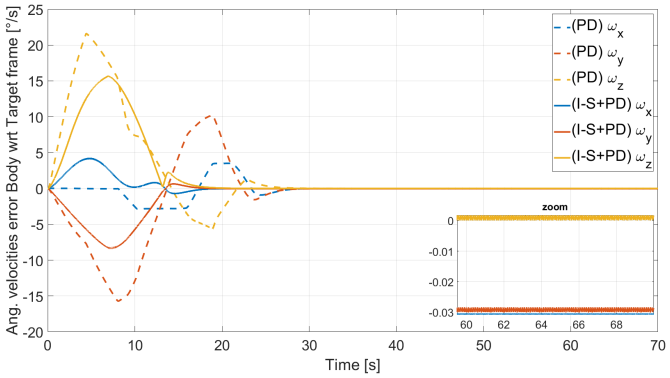

Figure 5: Case 4, angular velocities error Body w.r.t. Target frame. Comparison between PD and IDVD-SGRA+PD strategies.

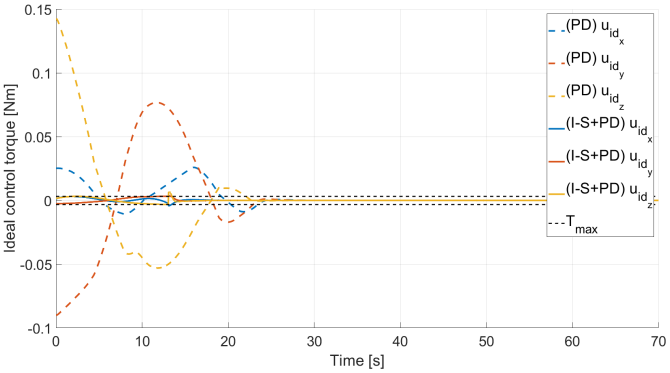

Figure 6: Case 4, requested control torque. Comparison between PD and IDVD-SGRA+PD strategies.

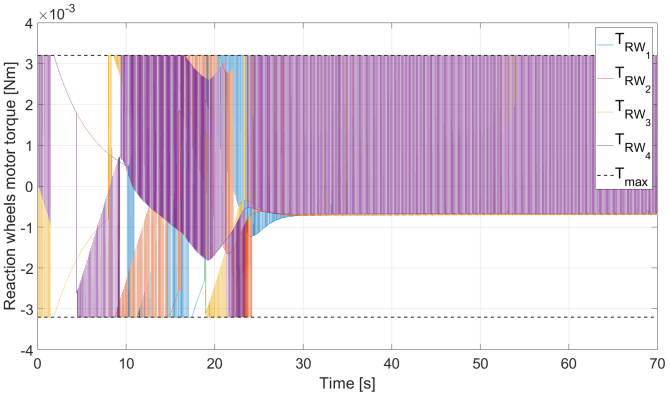

Figure 7: Case 4, actuated reaction wheels control torque (PD strategy).

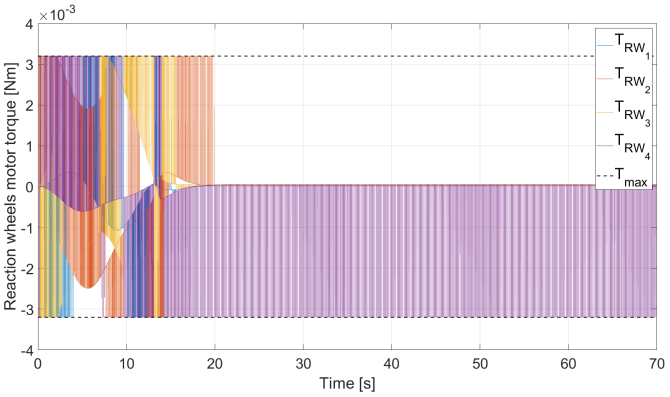

Figure 8: Case 4, actuated reaction wheels control torque (IDVD-SGRA+PD strategy).

V. Conclusions

From the analysis of the results, we can conclude that the IDVD-SGRA+PD guidance is always able to obtain settling times lower than the ones obtained with the standard PD controller. In the four cases studied, the proposed guidance is able to execute faster maneuvers than the conventional PD controller. In most cases, the settling time is 80% or smaller, a key advantage since the mission scenario requires to re-orient the S/C as fast as possible while satisfying the requirements on the pointing accuracy and on the maximum torque. Further improvement in the settling time and in the pointing accuracy can be reasonably reached if the IDVD-SGRA is implemented in a closed-loop fashion, and no need of PD controller to lock the pointing for the remaining part of the maneuver.

References

[1] George Boyarko, Marcello Romano, and Oleg Yakimenko. "Time-Optimal Reorientation of a Spacecraft Using an Inverse Dynamics Optimization Method". In: *Journal of Guidance, Control, and Dynamics* 34 (July 2011), pp. 1197–1208.

[2] Albert Caubet and James Biggs. "A motion planning method for spacecraft attitude maneuvers using single polynomials". In: *AAS/AIAA Astrodynamics Specialist Conference* (Aug. 2015).

[3] Xiaojiang Chen, Willem Steyn, and Y Hashida. "Ground-target tracking control of Earth-pointing satellites". In: *AIAA Guidance, Navigation, and Control Conference and Exhibit* (Aug. 2000).

[4] Marco Ciarcià, Alessio Grompone, and Marcello Romano. "A near-optimal guidance for cooperative docking maneuvers". In: *Acta Astronautica* 102 (Sept. 2014), pp. 367–377.

[5] Marco Ciarcià and Marcello Romano. "Suboptimal Guidance for Orbital Proximity Maneuver with Path Constraints Capability". In: *AIAA Guidance, Navigation, and Control Conference* (Aug. 2012).

[6] Howard D. Curtis. *Orbital Mechanics for Engineering Students*. Oxford: Elsevier, Butterworth-Heinemann, 2014.

[7] Karl D. Bilimoria and Bong Wie. "Time-optimal three-axis reorientation of rigid spacecraft". In: *Journal of Guidance Control Dynamics* 16 (May 1993), pp. 446–452.

[8] Abd El Hady M. Elbeltagy et al. "Fixed ground-target tracking control of satellites using a nonlinear model predictive control". In: *Mathematical Modelling of Engineering Problems* 5 (Mar. 2018).

[9] Zuliana Ismail and Renuganth Varatharajoo. "A study of reaction wheel configurations for a 3-axis satellite attitude control". In: *Advances in Space Research* 45.6 (2010), pp. 750–759.

[10] M. Kim, M. Kim, and S. Shin. "A general construction scheme for unit quaternion curves with simple high order derivatives". In: *Proceedings of the 22nd Annual Conference on Computer Graphics and Interactive Techniques* (1995), pp. 369–376.

[11] A. Miele, H. Y. Huang, and J. C. Heideman. "Sequential gradient-restoration algorithm for the minimization of constrained functions—Ordinary and conjugate gradient versions". In: *Journal of Optimization Theory and Applications* 4.4 (Oct. 1969), pp. 213–243.

[12] M.J. Sidi. *Spacecraft Dynamics and Control: A Practical Engineering Approach*. Cambridge (UK): Cambridge University Press, 1997.

[13] Willem H. Steyn. "A view finder control system for an earth observation satellite". In: *Aerospace Science and Technology* 10.3 (2006), pp. 248–255.

[14] J. Ventura, M. Romano, and U. Walter. "Performance evaluation of the inverse dynamics method for optimal spacecraft reorientation". In: *Acta Astronautica* 110 (May 2015), pp. 266–278.

[15] Jacopo Ventura et al. "Fast and Near-Optimal Guidance for Docking to Uncontrolled Spacecraft". In: *Journal of Guidance, Control, and Dynamics* 40 (Sept. 2016), pp. 1–17.

[16] J.R. Wertz. *Spacecraft Attitude Determination and Control*. Torrance (CA): Microcosm Inc., 1990.

[17] B. Wie. *Space Vehicle Dynamics and Control*. AIAA education series. American Institute of Aeronautics and Astronautics, 2008.

[18] Chang-Hee Won. "Comparative study of various control methods for attitude control of a LEO satellite". In: *Aerospace Science and Technology* 3 (July 1999), pp. 323–333.